Molecular-dynamics investigation of the desensitization of detonable material

Betsy M. Rice, William Mattson, and Samuel F. Trevino
Weapons and Materials Research Directorate, U.S. Army Research Laboratory, Aberdeen Proving Ground, Maryland 21005-5066
(Received 23 September 1997; revised manuscript received 15 December 1997)

A molecular-dynamics investigation of the effects of a diluent on the detonation of a model crystalline explosive is presented. The diluent, a heavy material that cannot exothermally react with any species of the system, is inserted into the crystalline explosive in two ways. The first series of simulations investigates the attenuation of the energy of a detonation wave in a pure explosive after it encounters a small layer of crystalline diluent that has been inserted into the lattice of the pure explosive. After the shock wave has traversed the diluent layer, it reenters the pure explosive. Unsupported detonation is not reestablished unless the energy of the detonation wave exceeds a threshold value. The second series of simulations investigates detonation of solid solutions of different concentrations of the explosive and diluent. For both types of simulations, the key to reestablishing or reaching unsupported detonation is the attainment of a critical number density behind the shock front. Once this critical density is reached, the explosive molecules make a transition to an atomic phase. This is the first step in the reaction mechanism that leads to the heat release that sustains the detonation. The reactive fragments formed from the atomization of the heteronuclear reactants subsequently combine with new partners, with homonuclear product formation exothermally favored. The results of detonation of the explosive-diluent crystals are consistent with those presented in an earlier study on detonation of pure explosive [B. M. Rice, W. Mattson, J. Grosh, and S. F. Trevino, Phys. Rev. E **53**, 611 (1996)].
[S1063-651X(98)09205-8]

PACS number(s): 82.40.Fp, 82.20.Wt, 03.40.Kf

I. INTRODUCTION

The process known as detonation has received considerable attention for its unique chemistry and physics and its military and industrial applications. Many explosives are well characterized at the macroscale and are adequately described at this level by hydrodynamic theories [1]. However, atomic-level details of detonation are not completely resolved, resulting in a gap in information that could otherwise be exploited in designing energetic materials with controlled detonation characteristics. This information includes features of the mechanisms of the chemical reactions and energy transfer that drive the detonation wave and conditions that affect these mechanisms. Much has been written concerning the first step in reactions of an explosive to produce a detonation wave [2,3]. Traditional views of the first step have assumed rupture of the weakest bond of the energetic molecule by thermal activation and/or mechanical stripping of fragments. Subsequently, the reactive species combine chemically and release energy to sustain the detonation. More recently, metallization has been invoked as a possible rate-controlling mechanism in the initial step [4]. Experimental data that could identify these various mechanisms are not available due to the small time and spatial scales over which detonation occurs. Typical detonation waves propagate through condensed media at speeds ranging from 1 to 10 km/s (1–10 nm/ps) and are currently outside the scope of experimental probe. Measurement is further complicated by the extreme energy and pressure release. The experimental community has made extensive progress toward measurement of detonation at subnanoscale regimes [3], but the necessary scale has yet to be reached.

Information at the microscale is readily obtained from molecular simulation. Through it the viewer observes and measures the dynamic events associated with detonation at the appropriate time and spatial scales. The motion of and force experienced by each particle in such a simulation can be monitored over time, allowing the investigator to witness reaction mechanisms. Several molecular-dynamics studies of shock-induced reaction waves in energetic molecular crystals show that detonation can be simulated using the method of molecular dynamics [5–23]. The main limitation of such studies to date, however, is the highly idealized representation of the energetic molecular system. Many common explosives are large polyatomic organic molecules and the reactions leading to detonation are thought to consist of several steps leading to the heat release that sustains the reaction wave. Most systems used in molecular simulations are simple di- and triatomic molecular crystals and the heat release reaction usually involves no more than two steps [5–23]. Despite these limitations, the simulations using such models have been extremely successful in reproducing characteristics of a detonation. In particular, the models of explosives developed by White and co-workers represent the chemistry thought to occur in detonation and explicitly include many-body effects [16]. These models, which use a modified Tersoff [24] form to describe the inter- and intramolecular interactions, have been successfully used to simulate chemically sustained reaction waves in crystals [15,16,18–23]. Such successes can be augmented by using information gained from simulations to design an energetic material with specific performance properties. The present study will explore this possibility using results from previous molecular-dynamics investigations of detonation [18,19]. It was found that the first step in the reaction sequence leading to detonation is the compression of the energetic solid to a critical density [18]. The simulations show that detonation will result if the critical density of the energetic material is

reached. A reasonable inference would be that the energetic material can be tailored such that this critical density will not be reached except under specific and controlled conditions. Tailoring toward desensitization could occur through the addition of inert dopants or defects, which would influence the degree of compression of the explosive due to shock wave passage. The work reported here will explore this hypothesis.

We present results from molecular-dynamics simulations that investigate the effect on detonation of an explosive by the addition of an inert heavy diluent. This diluent is inserted into the explosive crystal either in a layered fashion (slab simulations) or as part of a solid solution (solid solution simulations). The slab simulations investigate the conditions necessary for a ''slab'' of inert material inserted into the lattice to quench a detonation wave propagating through a pure explosive. The solid solution simulations investigate the behavior of mixtures of an explosive and a diluent after shock initiation. Finally, the dependence of detonation on the degree of compression of the material is determined.

II. MODEL

The models in this study are all two dimensional and consist of diatomic molecules arranged in herringbone lattices. The explosive molecules will be denoted hereafter as ''A-B'' and the diluent molecules will be denoted as ''C_2.'' All particles in the system will interact through the following interaction potential, a modified form of that developed in Ref. [16]:

$$V=\sum_{i}^{N}\sum_{j>i}^{N}\{f_c(r_{ij})[(2-\overline{B_{ij}})V_R(r_{ij})-\overline{B_{ij}}V_A(r_{ij})]+V_{\mathrm{vdW}}\}. \tag{1}$$

Parameters for the function and a description of the properties of this interaction potential are given in Refs. [18,19]. The V_R and V_A terms are functions that describe intramolecular repulsions and attractions, respectively. The V_{vdW} term describes nonbonding interactions. A many-body term, denoted as $\overline{B_{ij}}$, modifies the intramolecular interactions of a pair of atoms i and j according to the distribution of atoms surrounding the i-j pair. The value of $\overline{B_{ij}}$ ranges from 0 to 1 and depends only on the arrangement of atoms surrounding each atom pair. The value of $\overline{B_{ij}}$ does not depend on the atom type. The form of this potential attenuates the attractive intramolecular interaction and increases the repulsive interaction as an atom pair experiences an increasingly dense local environment, such as that occurring through shock wave passage. The previous study showed that in the reaction zone (the region behind the shock front in which the A-B molecules had not yet reacted) the density was such that the atom pairs making up each A-B molecule were experiencing no attractions [19]. Thus the molecules became ''unbound'' due to the compression of the material by passage of the pressure wave. Once the shock wave passed and the density of the region decreased, the attenuation of intramolecular attractions subsided and the nascent atoms were free to combine with new partners. For this system, homonuclear product formation is energetically favored and formation of such provides the energy needed to sustain the detonation wave.

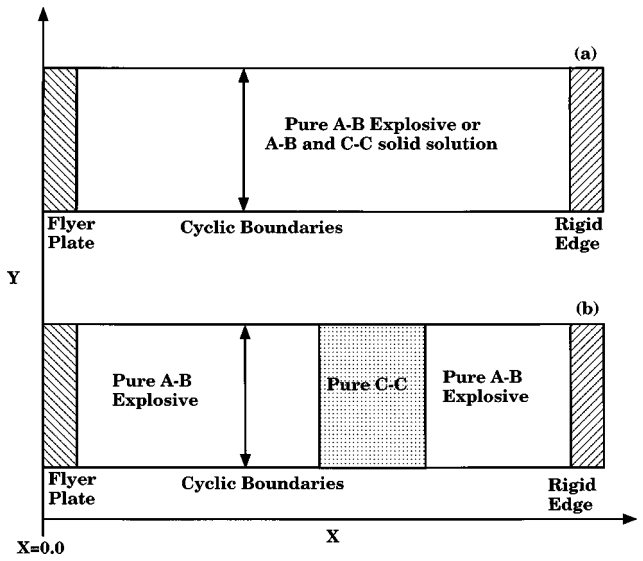

FIG. 1. Representations of lattice models used in the simulations: (a) pure explosive or solid solution and (b) pure explosive with a layer of diluent molecules inserted into the crystal lattice.

In the low-temperature, low-pressure crystal structure, bond strengths of the A-B, A_2, and B_2 molecules are 1, 5, and 2 eV, respectively. The C atom has the same interaction potential with all other species in the system as the A atom. The only difference between the C and A atoms is the mass. The mass of the C atom (150 amu) is ten times that of the A atom (15 amu). The bond strength of an isolated C_2 molecule is 5 eV, making it more stable than reactants by 4 eV. Also, the C_2 molecule has the same internuclear bond distance as the A_2 molecule (1.2 Å). The C_2 molecule can be dissociated with sufficient energy. However, there is no net energy change upon formation of C-A or recombination to form C_2. Also, formation of C-B is endothermic. Thus C_2 is appropriate as an ''inert'' diluent for desensitization of the model A-B explosive. The exothermic reactions for this system are

$$B\text{-}A+A\rightarrow B+A_2 \quad (\Delta E=-4.0 \text{ eV}),$$

$$A\text{-}B+B\rightarrow A+B_2 \quad (\Delta E=-1.0 \text{ eV}).$$

Due to the form of the interaction potential in Eq. (1), the C atom can influence the intramolecular interactions experienced by atom pairs in this system. Thus atom pairs within a mixture of a diluent and an explosive described by this form of potential-energy function will experience similar modifications of intramolecular forces upon compression as seen in the pure explosive.

III. DETAILS OF THE CALCULATIONS

Details of the molecular-dynamics simulations of the tailored explosives are the same as those described in Sec. III D of Ref. [18]. The most significant difference in the simulations is that the models do not consist of a pure explosive, but include the diluent C_2 molecules. Figure 1 represents the lattice models used in this study. For all simulations, all atoms in the simulation box are arranged in the local equilibrium position associated with the herringbone lattice. Atoms

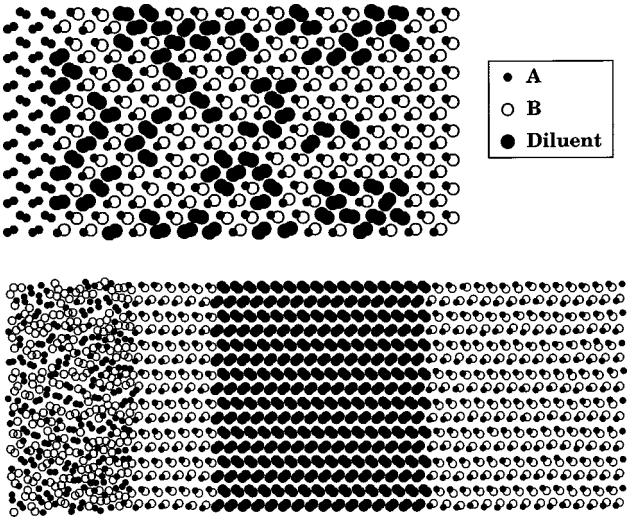

FIG. 2. Schematics of the models used in the molecular-dynamics simulations of explosive or diluent crystals. Atom type A (the mass equals 15 amu) is denoted by small filled circles, atom type B (the mass equals 46 amu) is denoted by open circles, and atom type C (the mass equals 150 amu) is denoted by large filled circles. The upper frame shows the solid solution of the initial positions of the explosive and diluent. The concentration of the diluent is 37.5%. The lower frame shows a snapshot of the layered explosive or diluent at 5.6 ps, immediately before the detonation wave reaches the left edge of the diluent region. The width of the diluent slab is 69 Å.

in the equilibrium herringbone arrangement are illustrated in Fig. 2. The upper frame of Fig. 2 shows the equilibrium herringbone lattice for a solid solution of the A-B explosive mixed with diluent C_2 molecules; the pure explosive crystal has the same atomic arrangement and differs only in the chemical composition (see Fig. 1 of Ref. [18]). Each atom is given kinetic energy totaling 20 K partitioned equally between the x and y momentum components. The equations of motion for the atoms in the simulation box are integrated for 0.05 ps to allow for randomization of the energy in the crystal. A shock wave is then initiated by the impact of a thin flyer plate consisting of 64 A_2 molecules moving at a velocity of 12 km/s. The earlier work showed that a flyer plate of this size, chemical composition, and velocity is sufficient to achieve steady detonation of the pure explosive [18]. The shock wave initiates at the far left edge of the simulation cell and propagates to the right. The model has cyclic boundary conditions in the y direction, but is terminated by a slab of rigid A-B molecules at the far right edge of the material. The model is not bound at the left edge, but can expand in the negative x direction as the flyer plate rebounds and the rarefaction occurs. The temperature of the crystal through which the shock wave will propagate is 20 K.

As in the previous study [18], the simulations here use the expanding computational window technique developed by Tsai and Trevino [5,6]. The temperature within an 8.68×50.16 Å^2 section of the crystal located 60.76 Å from the far-right edge of the terminating cell is monitored at each integration step. When the temperature within this ''test'' region exceeds that of the undisturbed crystal by 50%, it is assumed that the shock wave has propagated into this region. At that point, an 8.68×50.16 Å^2 section of crystal is inserted immediately before the rigid terminating cell. The atoms in the new segment are arranged in the equilibrium herringbone lattice position and energy totaling 20 K is partitioned into the x and y momentum components of each atom. The trajectory integration continues, with crystal added as needed to study wave propagation.

In the previous work [18], the shock front corresponded to the rightmost point along the x axis in which the mass density was greater than that of the undisturbed A-B crystal. This definition of shock front position is inadequate for this study since the mass density of the slab at the low pressure equilibrium (22.1 amu/Å^2) greatly exceeds that of the shocked A-B explosive (<10 amu/Å^2). For this study, the shock front is the rightmost 2.17×50.16 Å^2 section along the x axis of the model in which the average kinetic energy of the atoms exceeds 50 K. This prescription proved to be both more sensitive and stable than, say, using the number density.

A. Slab experiments

The first series of simulations exploits ideas used in measurements of explosive sensitivity known as ''gap tests'' [25]. These tests involve initiating a charge separated from the explosive being tested by an attenuating material. The shock wave produced from the initiating charge passes through the attenuating material before entering the sample explosive. The sensitivity of the explosive is defined in terms of the width of the attenuating material required for a 50% probability of initiation. Obviously, a slab of infinite width would completely attenuate the energy of the shock wave and the sample explosive would never detonate. The simulations reported in this work investigate the quenching of a detonation using such an attenuating material as a function of width.

The models consist of a pure A-B crystal except for a ''slab'' of material composed of C_2 molecules inserted into the explosive crystal. A pure explosive (with no defects) is on either side of the slab of the C_2 molecular crystal (Fig. 2). After flyer-plate initiation, detonation of the pure explosive is allowed to reach a steady state before the front reaches the slab of C_2 molecules. For each simulation, the shock front will reach the slab region 6.0 ps after shock initiation. The propagating detonation wave traverses the C_2 slab and then enters another region of the pure explosive. The reactions behind the shock wave after traversing the diluent region are monitored to decide if detonation is reestablished. Five simulations are performed that vary in the width of the slab of C_2 molecules. All of the slabs run the length of the simulation cell in the y direction (50.16 Å) and have periodic boundary conditions in that dimension. The differences in the sizes of the slabs are due to the width in the x direction. The widths of the slabs are 69.4, 86.8, 95.5, 104.2, and 138.9 Å. These simulations will be denoted hereafter by the width of the slabs, i.e., 69, 87, 95, 104, and 139.

B. Solid solution

The second set of computer simulations explores the response of explosive-diluent solutions upon flyer plate impact. The A-B explosive is mixed with the previously described C_2 molecules to form solid solutions. Three solutions

are chosen, with 31.25%, 34.375%, and 37.5% concentration of C_2 molecules. The simulations are denoted from now on by the concentration of C_2. The model of the solid solution is prepared as follows. The simulation cell at the beginning of the trajectory has dimensions of 69.44×50.16 Å^2. The cell is partitioned into rectangular sections with dimensions of 8.68×50.16 Å^2. A section of crystal with these dimensions can hold exactly 32 diatomic molecules in the low-pressure equilibrium herringbone lattice arrangement. The chemical composition of the 32 diatomic molecules (i.e., A-B or C_2) is assigned randomly according to the desired percent concentration of diluent molecules. Before the flyer plate is allowed to strike the edge of the simulation box of the explosive or diluent mixture, the system is allowed to relax through a 0.05-ps warm-up molecular-dynamics simulation. Energy redistribution and equipartitioning between the potential and kinetic energies are ensured by monitoring these during the warm-up trajectory. After the warm-up trajectory, the thin flyer plate of A_2 molecules moving with a velocity of 12 km/s strikes one edge of the solid solution. As the shock wave propagates into the undisturbed crystal, the simulation cell expands by the addition of a rectangular section of the solid solution, whose chemical composition has a fixed concentration of C_2 molecules arranged randomly as described previously.

IV. RESULTS

A. Slab simulations

The velocity of the shock wave of an unsupported detonation is a property of the explosive [1]. For the pure A-B explosive, the velocity of the detonation wave once a steady state has been reached is 6.6 km/s [18]. Thus the velocity of the shock wave through the explosive after traversing the slab of diluent is an indicator of whether detonation is reestablished. Figure 3 shows the positions of the shock fronts as functions of time for the simulations. The slopes of these curves correspond to the velocities of the propagating waves. The slope of each curve from 0.5 to 6 ps is 6.6 km/s. At 6 ps, the shock front enters the slab of C_2 molecules. The horizontal arrow in each frame of Fig. 3 shows the interval over which the shock front is in the slab of diluent molecules. The slope of each curve during this interval is less than that at the earlier interval of 0.5–6 ps, showing that the shock wave is propagating more slowly. The times in the trajectories at which the fronts reenter explosive are 7.8, 8.2, 8.4, 8.7, and 9.7 ps for the 69-, 87-, 95-, 104-, and 138-Å slab simulations, respectively. Linear least-squares fits of the curves from 12 to 15 ps give shock wave velocities of 6.8, 6.6, 6.7, 4.4, and 4.3 km/s for the 69-, 87-, 95-, 104-, and 138-Å simulations, respectively. The three simulations in which the shock velocities reach 6.6 km/s in the pure A-B explosive after traversing the diluent slab show that detonation is reestablished. Detonation of the A-B explosive did not resume after the shock wave traversed the slabs of C_2 molecules with widths of 104 and 138 Å.

Figures 4 and 5 show atomic number densities along the x axis at different times in the 104- and 95-Å simulations, respectively. As described in Ref. [18], a reactant A-B molecule is considered reacted if its internuclear distance exceeds 3.0 Å, the range of the intramolecular interaction potential. The designation of products in the figures merely means that the original A-B partners are no longer within the range of intramolecular interaction as defined by the function in Eq. (1). However, this test does not identify the products (homonuclear or heteronuclear diatomics or free atoms). Figure 4(a) shows atomic species profiles at 8.5 ps, soon after the time the shock front is reentering the pure explosive after traversing the C_2 slab. In Fig. 4(b) (0.5 ps later), no products have formed in the region beyond the diluent slab. In both Figs. 4(a) and 4(b), the diluent slab is compressed to ~75% of its low-pressure equilibrium width. The species profiles at 12 ps [Fig. 4(c)] show that the diluent slab has expanded to approximately its original width (104 Å) and a few products have formed in the region immediately to its right. However, the shock discontinuity is over 100 Å ahead of the location of the products and is followed by unreacted A-B molecules. The species profiles in Fig. 4(d) show that the distance between the positions of the shock discontinuity and the products along the x direction has increased over a 2.5-ps interval. Also, additional product has formed and the diluent slab has undergone further expansion. Product formation immediately ahead of the diluent slab is most likely due to the compression of the explosive on both sides. Compression from the left is due to expansion of the diluent slab after shock wave passage. Compression from the right is due to the disturbed A-B explosive, whose rarefaction is blocked by the heavy slab of diluent molecules. The compression of explosive results in the initiating step of reaction for this sys-

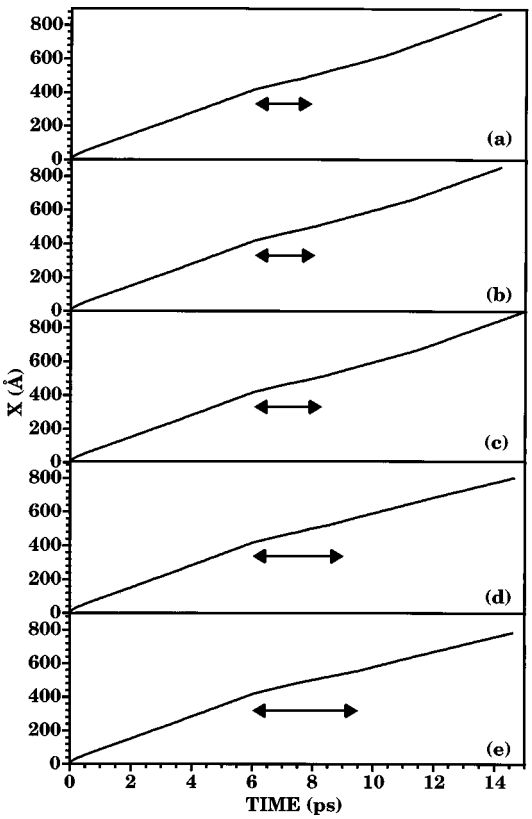

FIG. 3. Position of the shock front as a function of time for explosives with layers of diluent that have widths of (a) 69 Å, (b) 87 Å, (c) 95 Å, (d) 104 Å, and (e) 138 Å. The horizontal line in each frame illustrates the time interval of the trajectory over which the shock front is in the layer of diluent molecules.

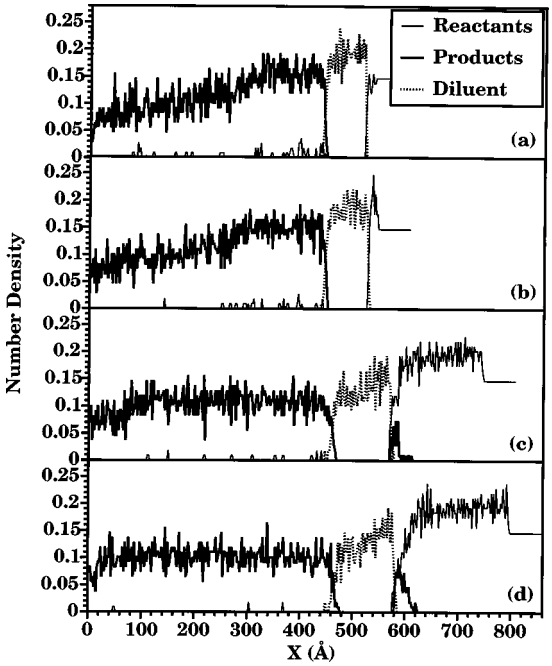

FIG. 4. Atomic number density as a function of position along the x direction of the model at (a) 8.5 ps, (b) 9.0 ps, (c) 12.0 ps, and (d) 14.5 ps. The low-pressure equilibrium width of the diluent slab in this simulation is 104 Å. Units are in $Å^{-2}$.

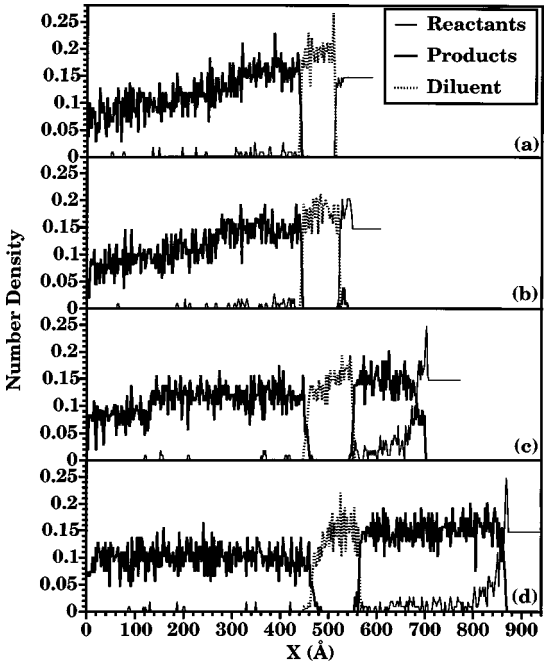

FIG. 5. Atomic number density as a function of position along the x direction of the model at (a) 8.5 ps, (b) 9.0 ps, (c) 12.0 ps, and (d) 14.5 ps. The low-pressure equilibrium width of the diluent slab in this simulation is 95 Å. Units are in $Å^{-2}$.

tem, i.e., atomization due to high density, followed by association to form exothermally favored homonuclear products. However, the heat release from product formation is apparently far enough behind the shock front that it does not contribute to continued propagation of the shock wave.

A similar series of species profiles for the trajectory in which the width of the slab of C_2 molecules is 95 Å is shown in Fig. 5. Figure 5(a) shows the profiles at 8.5 ps, near the point at which the shock wave is exiting the slab of C_2 molecules. The slab of diluent is compressed to $\sim$80% of its low-temperature, low-pressure equilibrium width. Figure 5(b) shows the species profile 0.5 ps later. Unlike the 104-Å trajectory at this point in the simulation, the diluent slab has expanded and a few products have formed immediately behind the shock front. Substantial product formation almost directly behind the shock discontinuity is evident at the later times [Figs. 5(c) and 5(d)] and the species profiles look similar to those corresponding to unsupported detonation in Ref. [18].

For those trajectories that reestablish detonation, the density behind the shock front reaches the Chapman-Jouguet value of the model explosive, which was shown in the previous work to be the key to achieving sustained detonation [18]. Examination of the results reveals that the critical density is not reached in the 104- and 138-Å simulations. For those cases, there is insufficient energy in the reentering shock wave to compress the explosive such that atomization and subsequent exothermic product formation will result. The energy of the detonation wave is attenuated as it traverses the heavy diluent region, transferring energy into the stationary, heavy C_2 molecules. Since there is no possibility of exothermic reaction within the diluent, there is no additional chemical energy released to drive the propagating wave in this region. By the time the shock wave reaches the far-right edge of the diluent region, it is moving with a slower velocity (therefore a smaller kinetic energy) than it had when it first entered that region. As shown in the flyer plate simulations of the pure explosive [18], there is a threshold energy needed to compress the pure explosive to the critical density. Apparently, a slab of diluent that is at least 104 Å wide is sufficient to dissipate the energy of the shock wave below the threshold value.

B. Solid solution simulations

Two of the three solid solutions (those with concentrations of 31.25% and 34.375% C_2 molecules) result in an unsupported detonation. In the previous work [18], detonation is sustained if the number density of the material behind the shock front in the pure explosive reaches 0.22 atom/$Å^2$ [26]. In the present study, solid solutions that attain this number density sustain detonation; the solid solution that did not achieve this value did not sustain detonation. Also, the reaction zones [27] for the two simulations that showed sustained detonation are 22–25 Å in width, $\sim$10 Å wider than that of the pure explosive [18]. A possible explanation for the increased reaction zone width is that product formation is sterically hindered by the presence of the diluent. In the shock compressed material, the C_2 molecules participate in atomization of the A-B molecules to form the reactive fragments [according to Eq. (1)]. However, exothermal association of the fragments of the reactant A-B molecules could be obstructed by C_2 molecules.

V. CONCLUSIONS

We have shown, using the method of molecular dynamics, simple ways in which a model explosive can be tailored

with a diluent to desensitize the material. The material was designed to exploit the reaction mechanism of the model, which is atomization of the explosive due to high compression, followed by the exothermal association of the fragments. Since the first step of the reaction involves high compression of the explosive, ways to attenuate the compression wave were introduced into the system. The first series of simulations investigated inserting slabs of inert heavy molecules into the explosive to absorb energy of the detonation wave. The attenuated shock wave, upon reentering explosive, has insufficient energy to achieve the critical compression necessary to atomize the reactant molecules.

The second series of simulations investigated the effect on detonation due to the mixture of a diluent with the explosive. The results showed that the diluent absorbs energy of the shock wave needed to compress the material to a critical density. The results also suggested that the diluent sterically hinders the reactive fragments from exothermic product formation. These two effects resulted in quenching the reactions that sustain the detonation.

This study has shown that results obtained from molecular dynamics can be used in the design of materials with specific performance objectives. The previously reported molecular-dynamics simulations of the pure explosive established the reaction mechanisms of the models [18,19], and the study reported here explored manipulations of the material to affect those reaction mechanisms. Clearly, microscale information obtained from this kind of modeling will become a useful and integral tool in the design and formulation of explosives with desired detonation characteristics.

[1] W. Fickett and W. C. Davis, *Detonation* (University of California Press, Berkeley, 1979); W. Fickett, *Introduction to Detonation Theory* (University of California Press, Berkeley, 1985).

[2] *Structure and Properties of Energetic Materials*, edited by D. H. Liebenberg, R. W. Armstrong, and J. J. Gilman, MRS Symposium Proceedings No. 296 (Materials Research Society, Pittsburgh, 1993).

[3] *Decomposition, Combustion and Detonation Chemistry of Energetic Materials*, edited by T. B. Brill, T. P. Russell, W. C. Tao, and R. B. Wardle, MRS Symposium Proceedings No. 418 (Materials Research Society, Pittsburgh, 1995).

[4] J. J. Gilman, Philos. Mag. B **67**, 207 (1993).

[5] D. H. Tsai and S. F. Trevino, J. Chem. Phys. **81**, 5636 (1984).

[6] D. H. Tsai, *Chemistry and Physics of Energetic Materials*, edited by S. N. Bulusu (Kluwer Academic, Dordrecht, 1990), pp. 195–227.

[7] M. Peyrard, S. Odiot, E. Lavenir, and J. M. Schnur, J. Appl. Phys. **57**, 2626 (1985).

[8] M. Peyrard, S. Odiot, E. Oran, J. Boris, and J. Schnur, Phys. Rev. B **33**, 2350 (1986).

[9] S. G. Lambrakos, M. Peyrard, E. S. Oran, and J. P. Boris, Phys. Rev. B **39**, 993 (1989).

[10] P. Maffre and M. Peyrard, Phys. Rev. B **45**, 9551 (1992).

[11] T. Kawakatsu, T. Matsuda, and A. Ueda, J. Phys. Soc. Jpn. **57**, 1191 (1988).

[12] T. Kawakatsu and A. Ueda, J. Phys. Soc. Jpn. **57**, 2955 (1988).

[13] T. Kawakatsu and A. Ueda, J. Phys. Soc. Jpn. **58**, 831 (1989).

[14] M. L. Elert, D. M. Deaven, D. W. Brenner, and C. T. White, Phys. Rev. B **39**, 1453 (1989).

[15] C. T. White, D. H. Robertson, M. L. Elert, and D. W. Brenner, in *Microscopic Simulations of Complex Hydrodynamic Phenomena*, edited by M. Mareschal and B. L. Holian (Plenum, New York, 1992), pp. 111–123.

[16] D. W. Brenner, D. H. Robertson, M. L. Elert, and C. T. White, Phys. Rev. Lett. **70**, 2174 (1993); **76**, 2202 (1996).

[17] L. Soulard, in *Decomposition, Combustion and Detonation Chemistry of Energetic Materials* (Ref. [3]), p. 293.

[18] B. M. Rice, W. Mattson, J. Grosh, and S. F. Trevino, Phys. Rev. E **53**, 611 (1996).

[19] B. M. Rice, W. Mattson, J. Grosh, and S. F. Trevino, Phys. Rev. E **53**, 623 (1996).

[20] P. J. Haskins and M. D. Cook, in *Proceedings of the American Physical Society Topical Conference on Shock Compression of Condensed Matter, Colorado Springs, 1993*, edited by S. C. Schmidt (AIP Press, New York, 1994), pp. 1341–1344.

[21] P. J. Haskins and M. D. Cook, in *Proceedings of the American Physical Society Topical Conference on Shock Compression of Condensed Matter, Seattle, 1995*, edited by S. C. Schmidt and W. C. Tao (AIP Press, Woodbury, New York, 1996), pp. 195–198.

[22] J. J. C. Barrett, D. H. Robertson, D. W. Brenner, and C. T. White, in *Decomposition, Combustion and Detonation Chemistry of Energetic Materials* (Ref. [3]), p. 301.

[23] C. T. White, J. J. C. Barrett, J. W. Mintmire, M. L. Elert, and D. H. Robertson, *Decomposition, Combustion and Detonation Chemistry of Energetic Materials* (Ref. [3]), p. 277.

[24] J. Tersoff, Phys. Rev. Lett. **61**, 2879 (1988); Phys. Rev. B **39**, 5566 (1989).

[25] Thomas N. Hall and James R. Holden, Navy Explosives Handbook ''Explosion Effects and Properties—Part III. Properties of Explosives and Explosive Compositions,'' Report No. NSWC MP-88-116, 1988 (unpublished).

[26] In Ref. [18], the analysis was performed in terms of mass density. In the present study, an analysis in terms of number density is more appropriate.

[27] In this work and in Ref. [18], the reaction zone is defined to be the region between the shock discontinuity and the point at which the number of products exceeds that of reactants.